Applied Surface Science xxx (2018) xxx–xxx

Contents lists available at ScienceDirect

Applied Surface Science

journal homepage: www.elsevier.com/locate/apsusc

Full Length Article

Enhanced photothermal bactericidal activity of chemically reduced graphene oxide stabilized by tripodal amphiphile

Ari Chae [a], Seongho Jo [a], Yujin Choi [a], Bowon Ryu [b], Cheong A. Choi [c], Sung Young Park [a,c,*], Insik In [a,d,*]

[a] Department of IT Convergence (Brian Korea PLUS 21), Korea National University of Transportation, 50 Daehak-ro, Chungju 380-702, Republic of Korea
[b] Division of Nano & Information Technology, KIST School, Korea University of Science and Technology, Seoul 02792, Republic of Korea
[c] Department of Chemical and Biological Engineering, Korea National University of Transportation, Chungju-Si 380-702, South Korea
[d] Department of Polymer Science and Engineering, Korea National University of Transportation, Chungju-Si 380-702, South Korea

ARTICLE INFO

Article history:
Received 1 November 2017
Revised 2 April 2018
Accepted 11 April 2018
Available online xxxx

Keywords:
Chemically reduced graphene oxide
Noncovalent interaction
Tripodal amphiphiles
Near infra-red absorbing
Photothermal
Bactericidal

ABSTRACT

Highly water-dispersible and strongly near IR absorbing chemically reduced graphene oxide (rGO)/CP750 assembly was firstly prepared through noncovalent approach from graphene oxide (GO) and CP750, a cyclotriphosphazene ring-based tripodal amphiphile. Through the stable noncovalent interaction by tripodal CP750 amphiphiles, rGO/CP750 assembly presented both high absorption coefficient of 2260 L g^{-1} m^{-1} and high near infrared (NIR) absorbance (1.07 at rGO concentration of 0.05 wt.%) in aqueous media without forming precipitates for a long term storage. Upon NIR laser (808 nm) irradiation, rGO/CP750 presented high photothermal heat generating ranging from +34.1 to +78.0 °C depending on the assembly concentration. Finally, excellent photothermal bactericidal performance of nearly 100% was accomplished toward both *E. coli* and *S. aureus* even at a low concentration of assembly (0.1 mg/mL) within 10 min of NIR irradiation. In overall, our study shows that high photothermal bactericidal performance that has been mainly claimed by other strongly NIR absorbing nanomaterials such as gold nanorods and semiconducting polymers can be easily accomplished from rGO-based nanomaterials with the proper utilization of tripodal amphiphiles.

1. Introduction

Solution-phase dispersion and stabilization of graphene or chemically reduced graphene oxide (rGO) in solvent media is tremendously important for many applications including optoelectrical devices, energy-harvesting devices, biomedical carriers, and nanocomposites to pursuit of advantages of wet processes based on soluble-processable graphene and its derivatives [1–3]. While several methods have been utilized for the formulation of stable graphene dispersion, the utilization of graphene oxide (GO) has additional benefits such as commercial availability, high dispersion concentration, wide range of surface modification tools, etc [4–6]. Either covalent or noncovalent approach has been attempted to provide soluble rGO but noncovalent approach has distinctive advantages due to its simplicity, no use of organic synthesis and purification, and no necessity of sp^3 linkages as defect sites, unavoidable in covalent approach [7–9]. Depending on the electronic characteristics of noncovalently interacting molecules or polymers on rGO sheets, either π-π interaction [10,11] and σ-π interaction [12–14] has been proposed to result in soluble and stable dispersion of rGO assembly (or hybrid) with interacting small molecules or polymers.

Numerous soluble rGO/polymer assemblies have been formulated by adopting noncovalent approach based on either π-π or σ-π interaction. However, σ-π interaction prevails π-π interaction due to wider applicability of σ-π interaction because noncovalently interacting polymers don't need the incorporation of π-conjugated structure [15–17]. However, van der Waals interaction between σ-rich polymers and π-rich rGO in σ-π interaction is often weakened and rGO precipitates are often produced in long-term storage of soluble rGO/polymer assembly through π-π stacking of neighboring rGO sheets. While various aliphatic polymers [12–15,17,18–21] and even amphiphilic block copolymers [23,24] have been utilized for the formulation of soluble rGO/polymer assemblies through this σ-π interaction, another stabilization strategy of soluble rGO assembly is required to enhance the kinetic stability of soluble rGO/polymer assembly in solution phase [17]. In the consideration of the above stability issue of rGO dispersion, the uti-

* Corresponding authors at: Department of Chemical and Biological Engineering and Department of IT Convergence (BK21 PLUS), Korea National University of Transportation, Chungju 27469, South Korea (S.Y. Park). Department of Polymer Science and Engineering and Department of IT Convergence (BK21 PLUS), Korea National University of Transportation, Chungju 27469, South Korea (I. In).
E-mail addresses: parkchem@ut.ac.kr (S.Y. Park), in1@ut.ac.kr (I. In).

https://doi.org/10.1016/j.apsusc.2018.04.119
0169-4332/

lization of amphiphilic block copolymer is much beneficial because hydrophilic segments stretch out to solvent media while hydrophobic segments anchor on inner hydrophobic rGO sheets. The presence of hydrophilic outer shell on inner rGO core definitely increases the kinetic stability of rGO dispersion as hydrophilic outer shell effectively hampers the facile π-π stacking of vicinal rGO sheets.

Until now, linear block copolymer amphiphiles such as Pluronic have been successfully utilized for the preparation of soluble rGO dispersion through σ-π interaction between them [22,23]. While this micellar stabilization of soluble rGO/Pluronic assembly is very effective for the solubilization and stabilization of rGO dispersion especially in aqueous media, the development of enhanced micellar stabilization of hydrophobic rGO dispersion by utilizing amphiphiles with different molecular structures and shapes is still very urgent. Specially, enhanced dispersion of rGO assembly by tripodal amphiphiles has not been developed in the previous literatures. Compared with their linear analogue, tripodal amphiphiles present enhanced micellar encapsulation for hydrophobic molecules such as doxorubicin, a cancer drug, together with prolonged dispersion stability in aqueous media [25–27]. The better performance of tripodal amphiphiles is regarded to originate from the formation of more dense hydrophobic or hydrophilic layers due to the molecular geometry of tripodal amphiphiles where three hydrophobic or hydrophilic segments parallely stretch out from the cyclotriphosphazene ring in the center into hydrophobic guests and aqueous media, respectively [27].

rGO-based nanomaterials showing excellent aqueous-phase dispersion and stabilization can be directly utilized as photothermal agents for photothermal therapy for various diseases [28–30]. As rGO/polymer assembly presents high optical absorption in near-infrared (NIR) region, photothermal heating effect of rGO-based materials is dramatically intensified and therefore enabling effective photothermal killing of bacteria [30–32]. While rGO itself has been tested as photothermal agents previously, hybridization of other strongly NIR-absorbing materials such as metal nanoparticles, semiconducting quantum dots, or conducting polymers is often attempted to increase the NIR absorbance of rGO-based hybrid nanomaterials [30,33,34]. However, little attention has been paid to enhance NIR absorption of rGO or rGO assembly itself. As a breakthrough, it has been demonstrated that optical absorption of rGO can be dramatically enhanced by controlling the lateral size distribution, the mean number of layers per flake, and the functional groups on rGO. Almost 3 orders of enhancement of absorption coefficient at 660 nm up to 6.72×10^6 L g m^{-1} was accomplished in rGO with a less amount of small flakes ($\leq$600 nm) and less layers per flake in *N*-methyl-2-pyrrolidone (NMP) [35]. However, rGO dispersion in NMP cannot be directly utilized as photothermal bactericidal agents and therefore the formulation of stable aqueous rGO dispersion with high absorption coefficient is highly encouraging.

Herein, we describe rGO dispersion with high stability and enhanced optical absorption coefficient in aqueous media without the use of other NIR absorbing substructures. With the utilization of CP750, a cyclotriphosphazene ring-based tripodal amphiphile, high optical absorption coefficient of 2260 L g m^{-1} was demonstrated in rGO/CP750 assembly. Through this high absorption coefficient, nearly 100% bacterial killing efficiency was accomplished toward both gram positive *E. coli* and gram negative *S. aureus* within 10 min of NIR irradiation even with a concentration of rGO/CP750 assembly as low as 0.1 mg/mL. This research highlights that the absorption coefficient, the resulting NIR absorbance, and the photothermal bactericidal activity of rGO/amphiphile assembly in the aqueous media are highly dependent on the structure of the amphiphiles. Moreover, the utilization of tripodal amphiphiles as graphene or rGO dispersing agent in the aqueous media can be used to maximize the optoelectrical performance of graphene and rGO in various applications.

2. Experimental

2.1. Materials and characterization

GO with a dimension of 5 μm and thickness of 1–2 nm was purchased from Daejoo Electronic Materials Co. (South Korea), and [N = P(MPEG750)(GlyPheLeu)Et]$_3$ (CP750) was synthesized according to a previous report [27]. GO and CP750 solution were freshly prepared just before use. Hydrazine monohydrate was purchased from Sigma-Aldrich Corp. (South Korea) and used without further purification. Anodized aluminum oxide (AAO) membrane with diameter of 47 mm and pore size of 0.2 μm was purchased from Fischer Scientific.

Ultraviolet–visible (UV–Vis) spectra of solution samples were obtained from Optizen α UV–Vis spectroscopy of Mecasys (South Korea). Fourier-transform infra-red (FT-IR) spectra were obtained from Nicolet Is10 spectrometer of Thermo Scientific and cumulated 16 scans at a resolution of 4 cm^{-1}. Raman analysis was done from ARAMIS dispersive Raman microscope of Horiba Jobin Yvon with the laser wavelength of 514 nm. Transmission electron microscopy (TEM) images were recorded with Tecnai TF30 ST of (FEI) at an accelerating voltage of 300 kV. Atomic force microscopy (AFM) images were obtained from XE-100 atomic force microscope of PSIA (South Korea). X-ray photoelectron spectroscopy (XPS) data were obtained from Sigma Probe of Thermo YG Scientific. The binding energy is accurate to within ±0.1 eV.

2.2. rGO/CP750 assembly

10 mg of CP750 was dissolved into 10 mL of distilled water and 1.0 mg of GO powder was dissolved into 10 mL of distilled water, respectively. Both solutions were mixed together and stirred for 24 h at room temperature, resulting in bright brown GO/CP750 mixture solution. Then, 100 μL of hydrazine monohydrate was added into GO/CP750 mixture solution and the overall reaction mixture was heated at 80 °C for 24 h, resulting in dark black rGO/CP750 assembly solution. To remove free CP750 from rGO/CP750 assembly solution and excess hydrazine, the resulting solution was centrifuged at 12,000 rpm (15,842 rcf) to settle down rGO/CP750 assembly in the bottom of conical tubes. After two times of washing with distilled water, rGO/CP750 assembly was again dispersed in deionized water. 15 mg of black-colored rGO/CP750 assembly powders were obtained after freeze drying of this solution at −50 °C.

2.3. Photothermal effect of rGO/CP750

An optical fiber-coupled 808 nm high-power diode laser (PSU-III-LRD, CNI Optoelectronics Technology Co. Ltd., Changchun, China) with power density of 2 W/cm^2 at a distance of 5 cm from the laser source was used to irradiate aqueous rGO/CP750 assembly solution with different concentrations in our experiments. For photothermal treatment, a laser beam with a diameter of 10 mm was focused on aqueous rGO/CP750 assembly solution. The distance between the NIR diode laser and vial of rGO/CP750 assembly solution was 5 cm in all tests. Infrared thermal images were taken with an NEC Avio Thermo Tracer TH9100 thermal imaging camera (South Korea).

Please cite this article in press as: A. Chae et al., Enhanced photothermal bactericidal activity of chemically reduced graphene oxide stabilized by tripodal amphiphile, Appl. Surf. Sci. (2018), https://doi.org/10.1016/j.apsusc.2018.04.119

2.4. Antibacterial activity

Stock solutions of *S. aureus* (Gram-positive, strain ATCC 25323) and *E. coli* (Gram-negative, strain ATCC 25922) were prepared in LB and MRS broth (50 mL) medium, respectively, and incubated at 37 °C for 12 h at 10^8 cells/mL with varying concentrations of rGO/CP750 assembly. At the end of the incubation period, *S. aureus* and *E. coli* strains treated either GO, GO/CP750 mixture, or rGO/CP750 assembly were irradiated with NIR laser for 1–10 min. The bacterial cells were then spread in Petri dishes for evaluation of the growth inhibition. Bactericidal effect was defined as a decrease in the CFU/mL after 24 h. For the control, both types of cells were used in the absence of rGO/CP750 assembly. The distance between the NIR diode laser and the bacteria solution was 5 cm, the irradiation area was 2 cm^2, and the solution volume was 0.2 mL.

3. Results and discussion

Efforts focusing specifically on the preparation of soluble rGO have utilized either water-soluble linear polymers such as carbomethoxy cellulose [36] and poly(*N*-vinyl pyridine) [17], or amphiphilic block copolymers such as Pluronic, poly(ethylene glycol)-*b*-poly(propylene glycol)-*b*-poly(ethylene glycol) copolymer [23]. CP750, a cyclotriphosphazene ring-based tripodal amphiphile, possesses three methoxy poly(ethylene glycol) (MPEG) as hydrophilic groups and three linear oligopeptides, $(GlyPheLeu)_2Et$, as hydrophobic groups on a phosphazene ring [25]. Through its unique morphology as a kind of tripodal amphiphiles, three hydrophilic MPEG and three hydrophobic oligopeptide groups are orienting in the same direction (Fig. 1a), which results in the facile formation of stable self-assembled micellar structures in aqueous solution with the critical micelle concentration (CMC) of 5.06 mg/L (1.13 μM) [27]. The reported CMC value of CP750 is dramatically lower than CMC values (10–100 mg/mL) of other linear amphiphilic diblock copolymers or even Pluronic. Because the micelle stability is tremendously affected on the CMC value and the interaction with hydrophobic guest molecules, it is highly encouraging to exploit the micellar stabilization of hydrophobic rGO by CP750, a representative cyclotriphosphazene ring-based tripodal amphiphile, in aqueous media.

3.1. Synthesis and characterization of rGO/CP750 assembly

Upon the incorporation of CP750 during the chemical reduction of GO by hydrazine as reducing agent, initially bright-brown colored GO/CP750 mixture solution changes to dark-black colored rGO/CP750 assembly solution. More importantly, prepared rGO/CP750 assembly solution is highly dispersible even after several months. No precipitation or floating particle is observed during the prolonged storage of prepared rGO/CP750 assembly solution. Comparison of UV–Vis spectra of both GO/CP750 mixture and rGO/CP750 assembly solutions clearly demonstrates the restoration of π-conjugated graphene lattices in rGO/CP750 assembly (Fig. 1b). The characteristic π-π^* transition peak of rGO was clearly observed at 271 nm, which is higher than π-π^* transition peak of GO at 236 nm and close to the highest wavelength reported as π-π^* transition peak of rGO [37]. Also importantly, significant increase of optical absorbance throughout the whole visible and NIR region (400–1100 nm) is observed. From the optical absorbance value at 660 nm, the absorption coefficient (ε) of rGO/CP750 assembly calculated from Beer–Lambert law is 2260 L g^{-1} m^{-1}, which is ×1.6 higher than 1390 L g^{-1} m^{-1} for graphite–water dispersions [38] and slightly less than 2460 L g^{-1} m^{-1} for graphite–NMP or graphite–dichlorobenzene dispersions [39,40]. Considering that CP750 doesn't have any optical absorbance at 660 nm, the above high absorption coefficient of rGO/CP750 assembly originates solely from rGO. Typically, rGO dispersions having a larger amount of big flakes reveal higher absorption coefficient at 660 nm. Therefore, the high absorption coefficient of rGO/CP750 assembly reminds us that the chemical reduction of GO to rGO and the simultaneous noncovalent attachment of hydrophobic oligopeptide groups of CP750 on rGO through noncovalent interaction (σ-π interaction or van der Waals interaction) don't result in the significant decrease in the lateral dimension of rGO plates, showing the effectiveness of CP750 as rGO-dispersing tripodal amphiphile. In addition, the optical absorbance of rGO/CP750 assembly (0.05 wt.%) at NIR region (808 nm) is 1.07, which is dramatically higher than 0.11 of pristine GO, which renders rGO/CP750 assembly to be applicable to an excellent candidate as photothermal agents enabling bacteria or cancer cell killing in biotherapy.

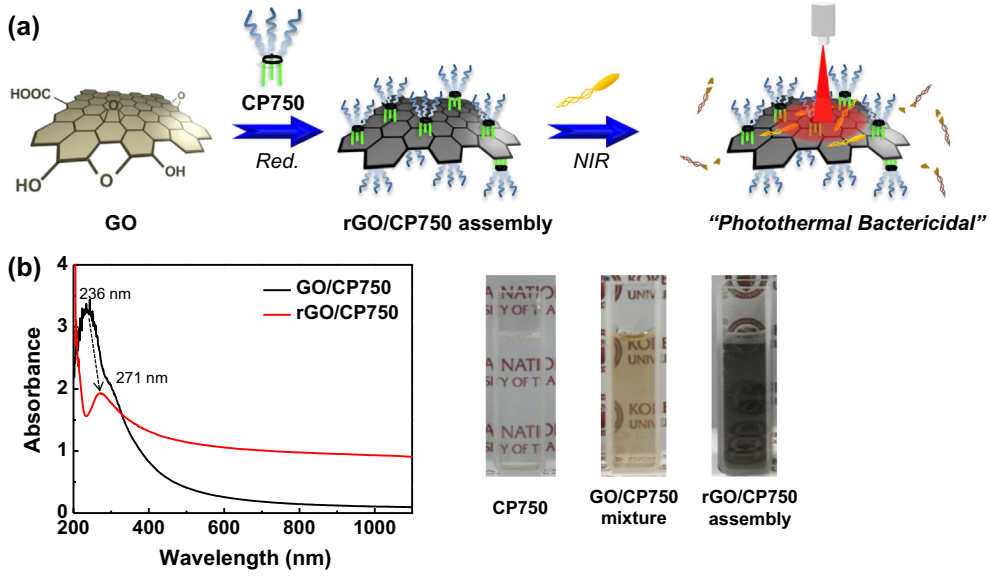

Fig. 1. (a) Illustration for the synthesis of rGO/CP750 assembly and its application as photothermal bactericidal agents and (b) UV–Vis spectra of both GO/CP750 mixture and rGO/CP750 assembly (the concentration of GO and rGO are 0.05 mg/mL) and photo images of aqueous solutions of CP750 (1 mg/mL), GO/CP750 mixture, and rGO/CP750 assembly.

Please cite this article in press as: A. Chae et al., Enhanced photothermal bactericidal activity of chemically reduced graphene oxide stabilized by tripodal amphiphile, Appl. Surf. Sci. (2018), https://doi.org/10.1016/j.apsusc.2018.04.119

The detailed morphology of rGO/CP750 assembly was examined by TEM and AFM. TEM images of rGO/CP750 assembly revealed the presence of ultrathin rGO plates as mostly single or few layered graphenes (Fig. 2a and b). More importantly, observed lateral dimension of rGO/CP750 assembly is not decreased compared with the lateral dimension of pristine GO (Fig. S1) after the simultaneous chemical reduction and noncovalent functionalization with CP750. AFM analysis of rGO/CP750 assemblies presented uniform thickness values of about 4.3 nm throughout all assemblies (Fig. 2c), revealing that rGO/CP750 assemblies possess single graphene sheet in each assembly surrounded with noncovalently attached CP750 amphiphiles [19]. The lateral dimension (hundreds nm) observed in AFM was slightly smaller than that (several μm) observed in TEM analysis. For FT-IR analysis, two types of samples were prepared. One is rGO films prepared by vacuum filtration of rGO/CP750 assembly solutions through AAO membrane and another is rGO/CP750 assembly powders isolated from the assembly solution by ultracentrifuge. As reported by the several previous literatures, σ-π interaction between π-rich rGO plates and σ-rich guest molecules is remarkably weakened during filtration process [12]. Therefore, FT-IR spectrum of rGO films revealed mostly features of rGO (Fig. 2d). C=O stretching peak of carboxylic acid groups of GO at 1741 cm^{-1} is mostly disappeared in rGO films [10]. The other sharp C—O stretching peaks at 1257 and 1118 cm^{-1} are preserved in rGO films, showing that the primary functional groups reduced during the chemical reduction process are carboxylic acid groups of GO. In the case of rGO/CP750 assembly powders, FT-IR spectrum of assembly powders presented the preservation of the characteristic peaks of CP750 [25,26], showing the presence of noncovalently interacting CP750 amphiphiles even in powder state (Fig. S2). Therefore, it is noteworthy that σ-π interaction between rGO and CP750 is robust both in solution state and the centrifuge process. Accordingly, while rGO films prepared by filtration are insoluble in aqueous media again, assembly powders are easily dispersed in water with simple agitation or brief sonication (Fig. S3). Again, the aqueous dispersion of rGO/CP750 assembly powders is highly stable for several months.

The structural and chemical information on the defects in rGO in the assembly can be exploited by Raman analysis [41]. Raman analysis of rGO films showed slightly increased D band to G band peak intensity ratio (I_D/I_G) of 1.10 compared with 0.92 of pristine GO powders (Fig. 3a). The position of D and G band peaks at 1350 and 1595 cm^{-1} is almost similar in both GO and rGO. The smaller increase of I_D/I_G in rGO films reveals again that the simultaneous chemical reduction and noncovalent functionalization of CP750 on rGO is not harmfully incorporating defect structures on prepared rGO in the assembly. Detailed atomic composition of the rGO/CP750 assembly was estimated by XPS analysis [14]. From the XPS full survey scans, rGO/CP750 assembly showed increased C to O ratio of 3.28:1 in their atomic-% (at.%) (Fig. 3b). In a comparison, GO showed C to O ratio of 2.25:1 in their atomic-% (at.%) (Fig. S4). The increase of relative amounts of carbon even in the presence of noncovalently interacting CP750 amphiphiles in rGO/CP750 assembly clearly reveals the successful chemical reduction from GO to rGO. Additionally, the presence of P (1.4 at.%) only in the XPS spectrum of the assembly powder shows the noncovalent

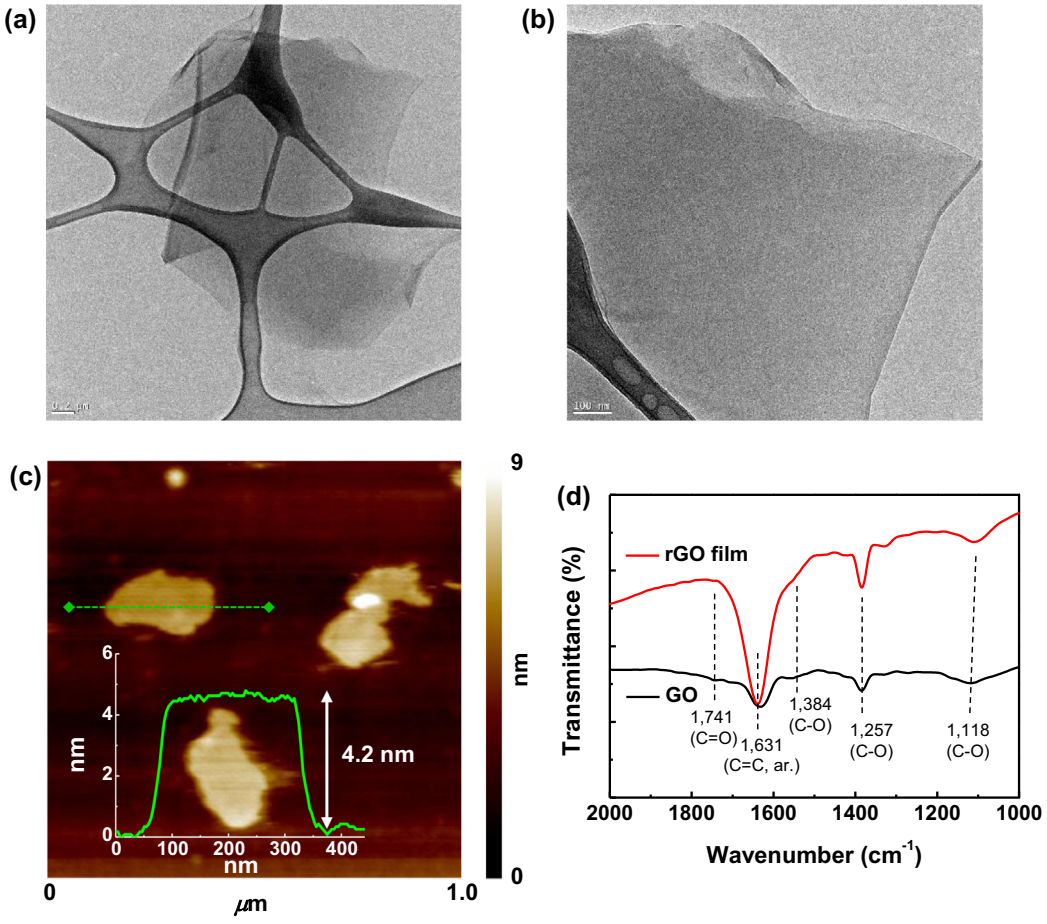

Fig. 2. (a) and (b) TEM images of rGO/CP750 assembly with different magnification, (c) AFM image of rGO/CP750 assembly on Si wafer (the height profile for selected dashed line), and (d) FT-IR spectra of GO and rGO film (prepared by vacuum filtration of rGO/CP750 assembly solution through AAO membrane).

Please cite this article in press as: A. Chae et al., Enhanced photothermal bactericidal activity of chemically reduced graphene oxide stabilized by tripodal amphiphile, Appl. Surf. Sci. (2018), https://doi.org/10.1016/j.apsusc.2018.04.119

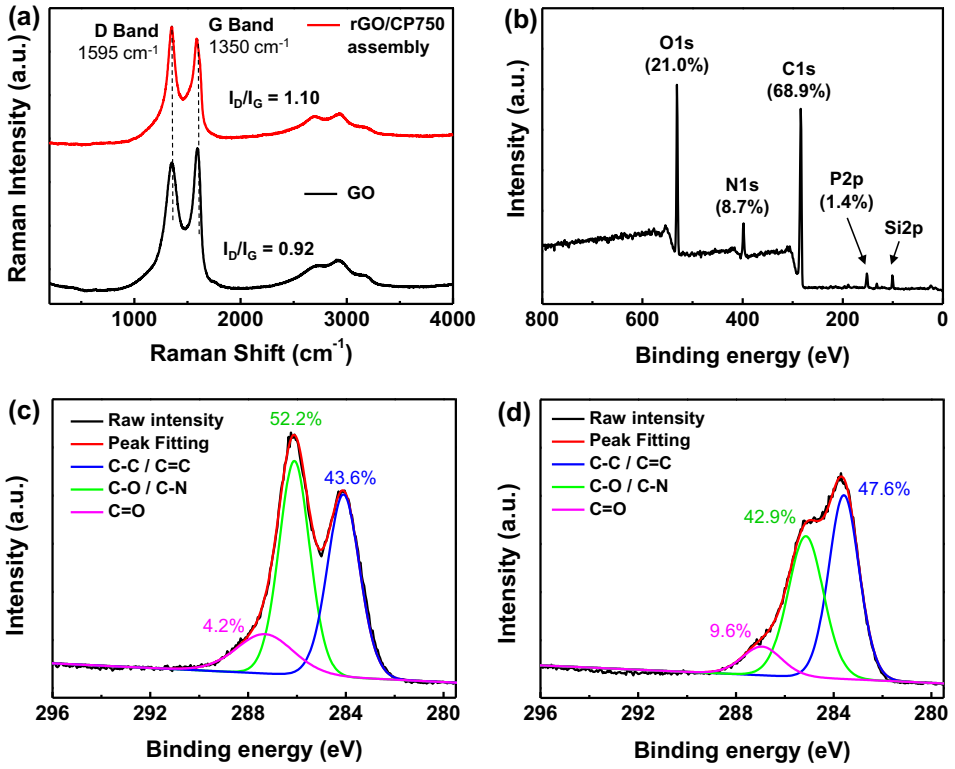

Fig. 3. (a) Raman spectra of both GO and rGO/CP750 assembly (powder), (b) XPS survey scan of rGO/CP750 assembly, and deconvoluted high resolution XPS C1s peaks of (c) GO and (d) rGO/CP750 assembly.

attachment of CP750 with cyclotriphosphazene ring ($[N = P]_3$) in the middle of its amphiphilic structure to rGO plates. The high inclusion of N (8.7 at.%) in the assembly originates from both N elements of oligopeptides of CP750 and hydrazine during the chemical reduction process. Also, deconvoluted C1s XPS binding peak of rGO reveals the slight increase of C=C binding portion in the rGO assembly compared with GO (Fig. 3c and d), which is corresponding with the increased C to O ratio in the assembly. Deconvolution of P2p binding peak of the assembly shows the inclusion of 84.5% of P—N/P=N bonding and 15.3% of P—O bonding at 132.1 and 133.1 eV, respectively, [42] which clearly confirms the presence of phosphazene ring structures of CP750 in the rGO assembly (Fig. S5).

3.2. Photothermal performance of rGO/CP750 assembly

The high optical absorption and dispersion stability of rGO/CP750 assembly are regarded to originate from the unique structure of CP750 as tripodal amphiphiles, which make the assembly to be ideal for a candidate as NIR absorbing photothermal agents. Upon NIR laser irradiation, aqueous solution of rGO/CP750 assembly showed 47.0 °C increase of solution temperature even at the low rGO/CP750 assembly concentration of 0.05 mg/mL (Fig. 4). Increase of rGO assembly concentration up to 0.5 mg/mL accomplished solution temperature of 94.6 °C (+77.6 °C increase from 17.0 °C before NIR laser irradiation). Therefore, it is clear that rGO/CP750 assembly is readily presenting photothermal heating effect on NIR laser irradiation. The dramatic NIR heating effects of assembly solutions result from rGO because CP750 itself doesn't induce noticeable heating effect on NIR laser irradiation. In the case of GO, slight photothermal heating effect is observed because GO also possesses isolated graphitic domains that could absorb NIR irradiation and release heat on the surrounding (Fig. S6) [43,44].

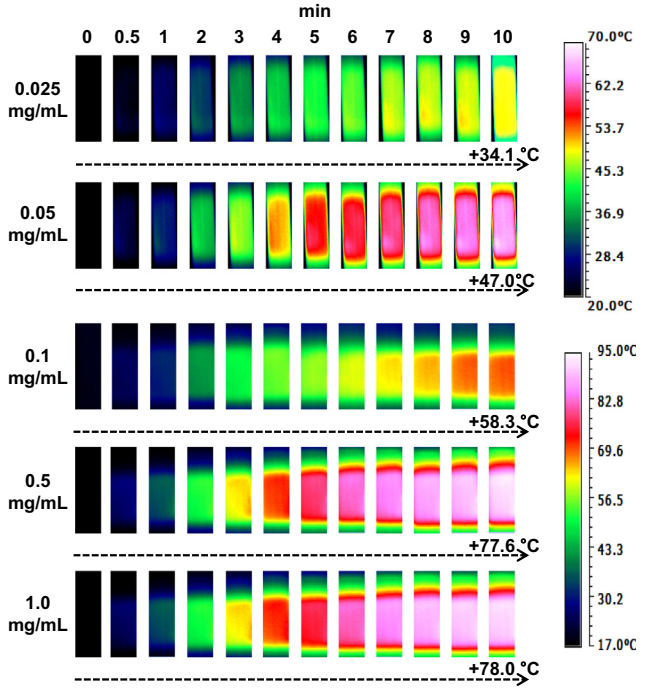

Fig. 4. (a) IR thermal images of rGO/CP750 assembly solutions in different concentrations upon the different NIR laser irradiation time.

3.3. Photothermal antibacterial performance of rGO/CP750 assembly

Then, bactericidal effects of rGO/CP750 assembly were evaluated toward both Gram-negative *E. coli* and Gram-positive *S. aureus* bacteria (Fig. 5). In the case of *E. coli*, rGO/CP750 assembly solu-

Please cite this article in press as: A. Chae et al., Enhanced photothermal bactericidal activity of chemically reduced graphene oxide stabilized by tripodal amphiphile, Appl. Surf. Sci. (2018), https://doi.org/10.1016/j.apsusc.2018.04.119

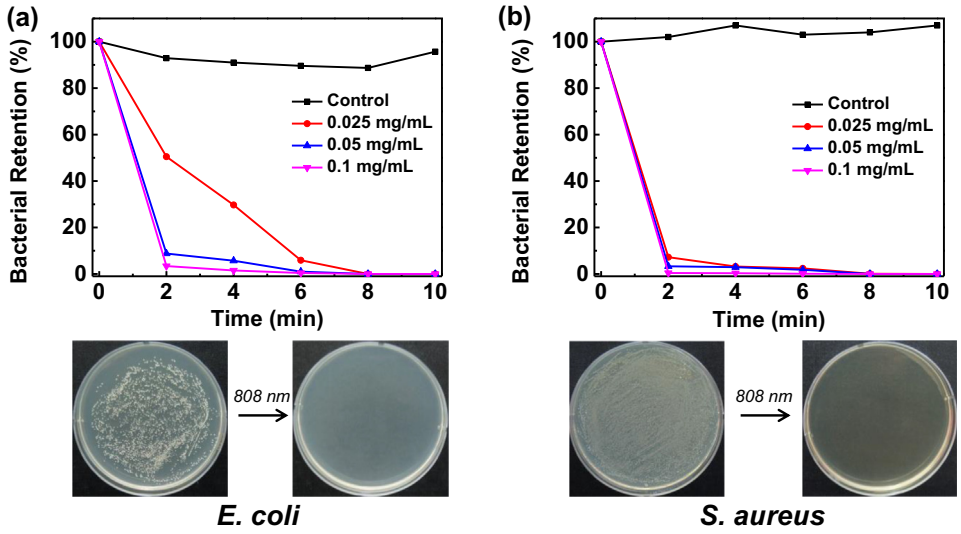

Fig. 5. Plots of bacterial retention of (a) *E. coli* and (b) *S. aureus* depending on the different NIR laser irradiation time (the bottom insets are the photo images of actual photothermal antibacterial event).

tions with concentration of either 0.1 or 0.5 mg/mL revealed 100% of bacteria killing efficiency after 8 min of NIR irradiation (Fig. S7). In the case of *S. aureus*, almost 100% bacteria killing efficiency was observed after 10 and 8 min of NIR irradiation in the assembly concentration of 0.1 and 0.5 mg/mL, respectively (Fig. S8). More importantly, rGO/CP750 assembly solutions demonstrate high bacterial killing efficiency more than 80% even just after 2 min of NIR laser irradiation for *E. Coli* (91.2% and 96.6% after 2 min with rGO/CP750 assembly concentration of 0.5 and 1.0 mg/mL, respectively) and *S. aureus* (92.8%, 96.7%, and 99.6% after 2 min with rGO/CP750 assembly concentration of 0.1, 0.5, and 1.0 mg/mL, respectively). Fast bactericidal activity of the assembly might originate from the high NIR absorbing performance of rGO/CP750 assembly together with the subsequent enhanced photothermal efficiency of the assembly. Photothermal conversion efficiency (η) of the assembly was evaluated by using the time constant method [45]. Through the obtained thermal time constants of 225.2 and 151.2 s of GO and rGO/CP750 assembly, respectively, the calculated η values of GO and rGO/CP750 assembly using the equation proposed by Roper were 2.3% and 7.5%, respectively (Fig. S9) [45,46]. The higher η value of rGO/CP750 assembly definitely originates from the high NIR absorbing performance of the assembly. Together with the high dispersion stability and strong NIR absorbing performance, rGO/CP750 assembly could be utilized for various future applications such as cancer treatment by hyperthermia [45–49].

4. Conclusions

Highly aqueous-dispersible and strongly NIR-absorbing rGO/CP750 assembly was developed by simple noncovalent approach. The unique compositional and morphological features of CP750 as tripodal cyclophosphazene-based amphiphile could result in the stabilization of rGO/CP750 assemby either in solution or solid state. With the irradiation of 808 nm NIR laser on aqueous dispersion of rGO/CP750 assembly (1.0 mg/mL), even temperature increase of +78.0 °C was accomplished. Therefore, bacterial killing efficiency of nearly 100% toward both Gram-negative *E. coli* and Gram-positive *S. aureus* was accomplished within 10 min of NIR laser irradiation even with the exploitation of low concentration of rGO/CP750 assembly such as 0.1 mg/mL. Our study reveals that soluble rGO/CP750 assembly can be successfully utilized as photothermal bactericidal agent even in the abscence of other strongly NIR-absorbing materials such as gold nanorods and conducting polymers, which enriches the direct bioapplication of soluble rGO assembly in many fields including photothermal bactericidal agents and possibly cancer treatment by hyperthermia.

Acknowledgements

This research was supported by Radiation Technology R&D program through the NRF funded by the Ministry of Science, ICT & Future Planning(NRF-2017M2A2A6A01019289), the Basic Science Research Program through the National Research Foundation of Korea (NRF) funded by the Ministry of Education (2015R1D1A3A01020192), and International Joint Technology Development Project (N0002123) through the Ministry of Trade, Industry and Energy (MI, Korea) and the Korea Institute for KIAT.

Appendix A. Supplementary material

Supplementary data associated with this article can be found, in the online version, at https://doi.org/10.1016/j.apsusc.2018.04.119.

References

[1] S. Stankovich, D.A. Dikin, G.H.B. Dommett, K.M. Kohlhaas, E.J. Zimney, E.A. Stach, R.D. Piner, S.T. Nguyen, R.S. Ruoff, Nature 442 (2006) 282–286.
[2] S. Park, R.S. Ruoff, Nat. Nanotechnol. 4 (2009) 217–224.
[3] R.V. Noorden, Nature 469 (2011) 14–16.
[4] D.R. Dreyer, S. Park, C.W. Bielawski, R.S. Ruoff, Chem. Soc. Rev. 39 (2010) 228–240.
[5] K.P. Loh, Q. Bao, G. Eda, M. Chhowalla, Nat. Chem. 2 (2010) 1015–1024.
[6] D. Chen, H. Feng, J. Li, Chem. Rev. 112 (2012) 6027–6053.
[7] J.M. Englert, C. Dotzer, G. Yang, M. Schmid, C. Papp, J.M. Gottfried, H.P. Steinruck, E. Spiecker, F. Hauke, A. Hirsch, Nat. Chem. 3 (2011) 279–286.
[8] V. Georgakilas, M. Otyepka, A.B. Bourlinos, V. Chandra, N. Kim, K.C. Kemp, P. Hobza, R. Zboril, K.S. Kim, Chem. Rev. 112 (2012) 6156–6214.
[9] J. Liu, J. Tang, J.J. Gooding, J. Mater. Chem. 22 (2012) 12435–12452.
[10] Y. Xu, H. Bai, G. Lu, C. Li, G. Shi, J. Am. Chem. Soc. 130 (18) (2008) 5856–5857.
[11] H. Yang, Q. Zhang, C. Shan, F. Li, D. Han, L. Niu, Langmuir 26 (9) (2010) 6708–6712.
[12] D.Y. Lee, Z. Khatun, J.H. Lee, Y.K. Lee, I. In, Biomacromolecules 12 (2011) 336–341.
[13] J.Y. Lee, Y.H. Park, A.K. Roy, B. Park, J.H. Jang, S.Y. Park, I. In, Chem. Lett. 44 (2015) 665–667.
[14] M. Lee, J. Lee, S.Y. Park, B. Min, B. Kim, I. In, Sci. Rep. 5 (2015) 11707–11716.
[15] L. Ren, T. Liu, J. Guo, S. Guo, X. Wang, W. Wang, Nanotechnology 21 (2010) 335701–335707.
[16] W. Wei, C. Xu, J. Ren, B. Xu, X. Qu, Chem. Commun. 48 (2012) 1284–1286.

[17] M.Y. Lee, S.H. Nam, J.Y. Lee, A.A. Nahain, S. Lee, C.M. Park, C.J. Han, S.Y. Park, I. In, J. Appl. Polym. Sci. 130 (4) (2013) 2538–2543.
[18] Y.J. Park, S.Y. Park, I. In, J. Ind. Eng. Chem. 17 (2011) 298–303.
[19] D.Y. Lee, S. Yoon, Y.J. Oh, S.Y. Park, I. In, Macromol. Chem. Phys. 212 (2011) 336–341.
[20] S. Yoon, I. In, J. Mater. Sci. 46 (2011) 1316–1321.
[21] J.Y. Lee, I. In, Chem. Lett. 41 (2012) 127–128.
[22] Y.J. Son, Y.H. Park, S.Y. Park, I. In, Chem. Lett. 44 (2015) 542–544.
[23] S.Z. Zu, B.H. Han, J. Phys. Chem. C 113 (2009) 13651–13657.
[24] G. Jeong, H.G. Kim, J.A. Nam, S.Y. Park, I. In, Chem. Lett. 42 (2013) 200–201.
[25] Y.J. Jun, U.S. Toti, H.Y. Kim, J.Y. Yu, B. Jeong, M.J. Jun, Y.S. Sohn, Angew. Chem. Ind. Ed. 45 (2006) 6173–6176.
[26] S.B. Lee, S.C. Song, J.I. Jin, Y.S. Sohn, J. Am. Chem. Soc. 122 (2000) 8315–8316.
[27] Y.J. Jun, V.B. Jadhav, J.H. Min, J.X. Cui, S.W. Chae, J.M. Choi, I.S. Kim, S.J. Choi, H.J. Lee, Y.S. Sohn, Int. J. Pharm. 422 (2012) 374–380.
[28] O. Akhavan, E. Ghaderi, A. Esfandiar, J. Phys. Chem. B 115 (2011) 6279–6288.
[29] M. Li, X. Yang, J. Ren, K. Qu, X. Qu, Adv. Mater. 24 (2012) 1722–1728.
[30] H. Ji, H. Sun, X. Qu, Adv. Drug Del. Rev. 105 (2016) 176–189.
[31] Y.W. Wang, Y.Y. Fu, L.J. Wu, Juan Li, H.H. Yang, G.N. Chen, J. Mater. Chem. B 1 (2013) 2496.
[32] M.C. Wu, A.R. Deokar, J.H. Liao, P.Y. Shih, Y.C. Ling, ACS Nano 7 (2) (2013) 1281–1290.
[33] D.K. Lim, A. Barhoumi, R. Wylie, G. Reznor, R. Langer, D.S. Kohane, Nano Lett. 13 (9) (2013) 4075–4079.
[34] K. Turcheniuk, C.H. Hage, J. Spadavecchia, A.Y. Serrano, I. Larroulet, A. Persquera, A. Zurutuza, M.G. Pisfil, L. Heliot, J. Boukaert, R. Boukherroub, S. Szunerits, J. Mater. Chem. B 3 (2015) 375–386.
[35] R. Su, S.F. Lin, D.Q. Chen, G.H. Chen, J. Phys. Chem. C 118 (2014) 12520–12525.
[36] S.G. Ha, Y.J. Yeon, S. Jung, Y.H. Park, B. Park, I. In, Chem. Lett. 42 (2013) 1409–1411.
[37] C.K. Chua, M. Pumera, Chem. Soc. Rev. 43 (2014) 291–312.
[38] M. Lotya, P.J. King, U. Khan, S. De, J.N. Coleman, ACS Nano 4 (6) (2010) 3155–3162.
[39] Y. Hernandez, V. Nicolosi, M. Lotya, F.M. Blughe, Z. Sun, S. De, I.T. Mcgovern, B. Holland, M. Byrne, Y.K. Gunko, J.J. Boland, P. Niraj, G. Duesberg, S. Krishnamurthy, R. Goodhue, J. Hutchison, V. Scardaci, A.C. Ferrari, J.N. Coleman, Nat. Nanotechnol. 3 (2008) 563–568.
[40] T. Hasan, F. Torrisi, Z. Sun, D. Popa, V. Nicolosi, G. Privitera, F. Bonaccorso, A.C. Ferrari, Phys. Status Solidi B 247 (2010) 2953–2957.
[41] K.N. Kudin, B. Ozbas, H.C. Schniepp, R.K. Prudhomme, I.A. Aksay, R. Car, Nano Lett. 8 (1) (2008) 36–41.
[42] S.K. Martha, J. Nanda, Y. Kim, R.R. Unocic, S. Pannala, N.J. Dudney, J. Mater. Chem. 1 (2013) 5587–5595.
[43] B. Tian, C. Wang, S. Zhang, L. Feng, Z. Liu, ACS Nano 5 (9) (2011) 7000–7009.
[44] W. Zhang, Z. Guo, D. Huang, Z. Liu, X. Guo, H. Zhong, Biomaterials 32 (2011) 8555–8561.
[45] Q. Tian, F. Jiang, R. Zou, Q. Liu, Z. Chen, M. Zhu, S. Yang, J. Wang, J. Wang, J. Hu, ACS Nano 5 (12) (2011) 9761–9771.
[46] O.A. Savchunk, J.J. Carvajal, J. Massons, M. Aguilo, F. Diaz, Carbon 103 (2016) 134–141.
[47] O. Akhavan, E. Ghaderi, S. Aghayee, Y. Fereydooni, A. Talebi, J. Mater. Chem. 22 (2011) 13773–13781.
[48] S. Kashyap, V. Kumar, S. Abraham, S. Umrao, S. Singh, A. Kamath, R. MS, A. Srivastava, P.S. Saxena, Austin J. Biosens. Bioelectron. 3 (1) (2017) 1026–1030.
[49] E.B. Kang, I. In, K.D. Lee, S.Y. Park, J. Ind. Eng. Chem. 55 (2017) 224–233.

Please cite this article in press as: A. Chae et al., Enhanced photothermal bactericidal activity of chemically reduced graphene oxide stabilized by tripodal amphiphile, Appl. Surf. Sci. (2018), https://doi.org/10.1016/j.apsusc.2018.04.119